

**SYNTHESIS AND CHARACTERIZATION OF  $\text{Ba}_{0.8}\text{Sr}_{0.2}\text{TiO}_3\text{-Co}_{0.8}\text{Zn}_{0.2}\text{Fe}_2\text{O}_4$   
MULTIFERROIC COMPOSITES PREPARED BY SOLID STATE REACTION  
METHOD**

A THESIS SUBMITTED IN PARTIAL FULFILLMENT  
OF THE REQUIREMENTS FOR THE DEGREE OF

**BACHELOR OF TECHNOLOGY  
IN CERAMIC ENGINEERING**

BY

**RANJAN KR PANDA**

111CR0569

under the guidance of

**Prof. Arun Chowdhury**



**DEPARTMENT OF CERAMIC ENGINEERING  
NATIONAL INSTITUTE OF TECHNOLOGY  
ROURKELA - 769008  
2014-152015**

SYNTHESIS AND CHARACTERIZATION OF  $\text{Ba}_{0.8}\text{Sr}_{0.2}\text{TiO}_3\text{-Co}_{0.8}\text{Zn}_{0.2}\text{Fe}_2\text{O}_4$   
MULTIFERROIC COMPOSITES PREPARED BY SOLID STATE REACTION METHOD

A THESIS SUBMITTED IN PARTIAL FULFILLMENT  
OF THE REQUIREMENTS FOR THE DEGREE OF

**BACHELOR OF TECHNOLOGY  
IN CERAMIC ENGINEERING**

BY  
**RANJAN KAMAR PANDA**  
111CR0569

Under the guidance of

**Prof. Arun Chowdhury**



**DEPARTMENT OF CERAMIC ENGINEERING  
NATIONAL INSTITUTE OF TECHNOLOGY  
ROURKELA – 769008  
2014-15**

## CERTIFICATE

This is to certify that the thesis entitled, “SYNTHESIS AND CHARACTERIZATION OF  $\text{Ba}_{0.8}\text{Sr}_{0.2}\text{TiO}_3\text{-Co}_{0.8}\text{Zn}_{0.2}\text{Fe}_2\text{O}_4$  MULTIFERROIC COMPOSITES PREPARED BY SOLID STATE REACTION METHOD” submitted by **Mr. Ranjan Kumar Panda** in partial fulfillment of the requirements of the award of Bachelor of Technology Degree in Ceramic Engineering at the National Institute of Technology, Rourkela is an authentic work carried out by him under my supervision and guidance.

To the best of my knowledge, the matter embodied in the thesis has not been submitted to any other university / institute for the award of any Degree or Diploma.

Date: 26.06.2015

**Prof. Arun Chowdhury**

Dept. of Ceramic Engineering

National Institute of Technology  
Rourkela – 769008

## ACKNOWLEDGEMENT

It gives me immense pleasure to express my deep sense of gratitude to my supervisor **Prof. Arun Chowdhury** for his invaluable guidance, motivation, constant inspiration and above all his ever co-operating attitude enabled me in bringing up this thesis in present elegant form.

I am extremely thankful to **Prof. S. K. Pratihari** Head, Department of Ceramic Engineering and the faculty members of Ceramic Engineering Department for providing all kinds of possible help and advice during the course of this work.

It is a great pleasure for me to acknowledge and express my gratitude to my parents for their understanding, unstinted support and endless encouragement during my study.

I am greatly thankful to all the staff members of the department and all my well-wishers, class mates and friends for their inspiration and help.

Lastly I sincerely thank to all those who have directly or indirectly helped for the work reported herein.

RANJAN KUMAR PANDA

ROLL NO: 111CR0569

Department of Ceramic Engineering  
National Institute of Technology, Rourkela

## List of figures

<b>NAME OF THE FIGURES</b>	<b>PAGE NO</b>
<b>1.XRD graph of calcined BST prepared by solid state reaction (1000 °C)</b>	<b>23</b>
<b>2. XRD graph of <math>\text{Co}_{0.8}\text{Zn}_{0.2}\text{Fe}_2\text{O}_4</math> synthesized by solid state reaction</b>	<b>24</b>
<b>3. XRD pattern of pellets after preparation from mixed batches</b>	<b>24</b>
<b>4. XRD of pellets sintered at 1175 °C (mixing+15 minutes sonication )</b>	<b>25</b>
<b>5. .XRD pattern of pellets after 30 min sonication</b>	<b>27</b>
<b>6. FE-SEM images of 0.6BST-0.4CZF after 1175 °C/2hr (without sonication)</b>	<b>28</b>
<b>7. FE-SEM images of 0.6BST-0.4CZF after 1175 °C/2hr ( 15 min sonication</b>	<b>29</b>
<b>8. FE-SEM images of 0.6BST-0.4CZF after 1175 °C/2hr ( 30 min sonication)</b>	<b>31</b>
<b>9. dilatometric curve of three green compacted compositions</b>	<b>33</b>
<b>10. B-H loops of three composites only mixed in agate</b>	<b>34</b>
<b>11. B-H loops of three composites mixed in agate followed by 15 min dispersion</b>	<b>35</b>
<b>12. B-H loops of three composites mixed in agate followed by 30 min dispersion</b>	<b>36</b>
<b>13. P-E loops of three composites mixed in agate only</b>	<b>38</b>

## LIST OF TABLE

<b>NAME OF THE TABLE</b>	<b>PAGE NO</b>
<b>1 previous work on synthesis of CZF</b>	<b>16</b>
<b>2.Previous works on synthesis of BST</b>	<b>17</b>
<b>3. average grain size of BST and CZF</b>	<b>30</b>
<b>4. average grain size of BST and CZF of pellets (mixing in agate + 15 min sonication)</b>	<b>31</b>
<b>5. : B.D. data of pellets sintered at 1175 °C/2hr</b>	<b>33</b>
<b>6. Onset temperature of densification (°C) mixed in agate only</b>	<b>35</b>
<b>7.Magnetic order parameters as obtained from B-H loops</b>	<b>38</b>
<b>8. : Ferroelectric order parameters as obtained from P-E loops</b>	<b>39</b>

## **ABSTRACT**

The magnetic material is now very much used in the various purposes. They are also used in the electrical application. In this paper we have studied the various characteristics like magnetic, structural and other physical properties of barium strontium titanate-cobalt zinc ferrite prepared by the solid state method. The crystal structure or phase is studied by XRD. Zinc and strontium ion is substituted about 20 percent in place of cobalt and barium respectively. The composites prepared in 60:40, 70:30, 80:20 percent respectively. The sintering behavior is studied at different temperature. Microstructure also analysis using FESEM. Thermal expansion is studied using dilatometer. During preparation of  $\text{Ba}_{0.8}\text{Sr}_{0.2}\text{TiO}_3$  and  $\text{Co}_{0.8}\text{Zn}_{0.2}\text{Fe}_2\text{O}_4$  by solid route method they were calcined at  $900^\circ\text{C}$  for two hours and  $950^\circ\text{C}$  for one hour respectively. Then the sample are mixed by isopropyl alcohol and dried. Pellet were made and fired at  $1175^\circ\text{C}$  and characterization were studied.

## **Contents**

Serial No.

Pages

- 1) Chapter 1: Introduction
- 2) Chapter 2: Literature Review
- 3) Chapter 3: Experimental Procedure
- 4) Chapter 4: Results and discussions
- 5) Chapter 5: Conclusions
- 6) Chapter 6: References



Chapter 1:

# **INTRODUCTION**

### **Barium Strontium titanate:**

**Chemical formula= $\text{Ba}_{0.8}\text{Sr}_{0.2}\text{TiO}_3$**

Barium Strontium titanate (BST) is ceramic material which is the solid solution of barium titanate and strontium titanate. It is a ferroelectric material having perovskite structure as per the structure of barium titanate and strontium titanate. This solid solution is formed by the method of doping. In doping process some amounts of barium ions ( $\text{Ba}^{2+}$ ) are replaced by strontium ions ( $\text{Sr}^{2+}$ ) thus forming the solid solution of barium strontium titanate. In this process the lattice parameter is slightly changed as compared to barium titanate. The BST is generally prepared by different methods like auto combustion, sol-gel, precursor methods etc. For all the cases the properties of the powder will be same. BST is also known as the piezoelectric material which is derived from  $\text{BaTiO}_3$  which is a piezoelectric material. The “A” site ion of  $\text{BaTiO}_3$  is replaced by a di valence cation i.e.,-Sr. Due to the vacancy of the donor dopant the soft piezoelectric is generated. That’s why BST is a soft piezoelectric material also. BST is generally used for electronic industries for the following properties-

- Dielectric constant (1164) is high as compared to  $\text{BaTiO}_3$
- Low dielectric loss (0.063)
- Low leakage current density ( $49.4 \text{ pA/cm}^2$ )
- High breakdown strength
- Good thermal stability

Apart from that BST is used for manufacture of ceramic capacitor, under cooler detector fabrication, photorefractive mirrors and a gate insulators of the oxide superconductors FET in the thin films. Also BST is used in actuators, hydrophones, SONAR devices etc. for its excellent piezoelectric properties and compatibility.

## **Cobalt Zinc ferrite:**

**Chemical formula=** $\text{Co}_{0.8}\text{Zn}_{0.2}\text{Fe}_2\text{O}_4$

Now-a-days the magnetic materials play a significant role in both from fundamental and applicable point of view. Recently the new magnetic ceramics play a vital role in the application areas due to their high permittivity, low hysteresis loss, low temperature dependence of magnetic field intensity etc.. The ceramics which are used as magnetic materials are generally spinel ferrites having excellent magnetic and electrical properties. There are different spinel structures like normal spinel and inverse spinel.  $\text{CoFe}_2\text{O}_4$  is most used ferromagnetic ceramics used as magnetic materials due to its cubic magneto crystalline anisotropy, high coercivity, moderate saturation magnetization, and high chemical stability magnetic and electrical conductivity.

The general formula of normal spinel is  $\text{AB}_2\text{O}_4$  where A represents the tetrahedral interstices and B represents the octahedral interstices. It has a face centered cubic structure with a large unit cell containing 8 formula unit cells. From the resulting 64A sites and 32B sites only 8 and 16 are occupied. The variation of cation distribution over the A and B sites in the spinel ferrite leads to different magnetic properties.

But in inverse spinel the general formula is  $\text{BABO}_4$  where half of the tetrahedral sites will be filled by the B sites.  $\text{CoFe}_2\text{O}_4$  is an inverse spinel where half of the Fe atom occupy the tetrahedral sites. When we incorporate some of the Zn atom to that spinel then the lattice parameter is changed along with the structure is changed to distorted spinel structure. It has been experimentally observed that with increase in particle size of cobalt zinc ferrite magnetization decrease. It has also been observed that the substitution of  $\text{Zn}^{2+}$  with  $\text{Co}^{2+}$  lead to improve magnetic properties with some extent and decreases the saturation magnetization with increase of Zn content after a certain percentage of Zn.

### **Properties of Cobalt Zinc ferrite**

- Ferromagnetic material
- Piezomagnetic material
- Hard magnetic material
- Lattice parameter=0.840nm
- Density = 5.21gm/cc

### Uses of Cobalt Zinc ferrite

- Ferro fluid
- Magnetic drug delivery
- Hyper thermia for cancer treatment
- Magnetic storage etc...

The magnetic material are very important as it is very much used in electronic equipment such as hard disk drive, motor, actuator, and sensor.

With the advancement of electronic innovation, composite materials have been broadly utilized for electronic gadgets where higher densities, constrained space and multifunction are needed. As of late the ferroelectric–ferromagnetic composite materials were seriously inquired about for two uses: the magnetic–electric sensors in radio-gadgets, optoelectronics, microwave hardware and transducers and the minimized electrical channels for smothering electromagnetic impedance (EMI). With respect to the magnetic–electric sensors, high ferroelectric substance was essential for the composite materials with adequate resistivity to produce magneto electric impact.

In the previous couple of years, broad exploration has been led on magneto electric impact in single stage and composite materials. Direct polarization of a material under an attractive field or an in incited charge under an electric field requires the synchronous vicinity of long range requesting of attractive minutes and electric dipoles.

Magneto Electric materials are of two types:

- Single Phase
- Composites

In a magneto electric (ME) composite the magnetostrictive strain in the attractive stage makes an electric polarization in the contiguous piezoelectric stage and thus is equipped for changing over attractive field into electric field and the other way around. Such property can be used in materials utilized as a part of sensors, processors and input frameworks.

Magneto electric composites on other hand have vast magneto electric coefficients of size of magneto electric voltage coefficients. The composites are made misusing the item property of material. Composite materials are engineered materials made from two or more constituent materials with significantly different physical or chemical properties and which remain separate and distinct on a macro space level within the finished structure.

Multi ferric materials display more than one essential ferric request parameter, for example, Ferro/antiferromagnetic, Ferro electricity, Ferro versatility in a solitary stage.

### **Other Magneto electric Applications:**

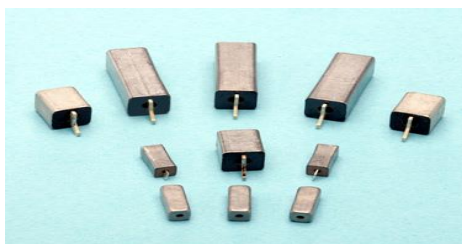
- SENSORS



- TRANSDUCERS



- MICROWAVE DEVICES



Chapter 2:

**LITERATURE**

**REVIEW**

Historically BaTiO<sub>3</sub>- CoFe<sub>2</sub>O<sub>4</sub> composites were first obtained in 1972 by Van Suchtelen.

Type of materials that undergo ME multiferroic: Single material/ Composite

Theoretically the magneto electric effect came into picture in 1894 when Curie discussed correlation of magnetic and electric properties in low symmetry crystals. Another strong footing on ME effect theoretically is by L.D. Landau in 1957. According to him, “The magneto electric effect is odd with respect to time reversal and vanishes in materials without magnetic structure. First experimental observation of the ME effect was in 1960 by Astrov who found the electric field induced magneto electric effect in Cr<sub>2</sub>O<sub>3</sub>. One year later the reverse effect in same system was observed by Rado et al. The BaTiO<sub>3</sub>- CoFe<sub>2</sub>O<sub>4</sub> composite was first prepared by unidirectional solidification of BaTiO<sub>3</sub>- CoFe<sub>2</sub>O<sub>4</sub> eutectic liquid. Van such élan was the pioneer and he introduced the product properties. Among various magneto electric composite systems, BaTiO<sub>3</sub> / CoFe<sub>2</sub>O<sub>4</sub> composite materials are first investigated. The unidirectional solidification lets the composite to come up with a lamellar morphology. The phases as Co<sub>2</sub>TiO<sub>4</sub> and (BaFe<sub>12</sub>O<sub>9</sub>)<sub>y</sub> (BaCo<sub>6</sub>Ti<sub>6</sub>O<sub>19</sub>)<sub>1-y</sub> could also exist in the system. The resulting lamellar microstructure prevents the relatively conductive CoFe<sub>2</sub>O<sub>4</sub> phase from forming conducting chains along the poling directions. Consequently the composite materials possess a relatively high ME sensitivity (30 mV/cm-Oe) but the unidirectional solidification process is not easy to be implemented. Solid state reaction or conventional ceramics method is usually followed to prepare BaTiO<sub>3</sub>- CoFe<sub>2</sub>O<sub>4</sub> or BaTiO<sub>3</sub>- CoFe<sub>2</sub>O<sub>4</sub> based composites. The advantages of this route are: simple, cheap and free choice of composition of the constituents. Using this method various composites have been made such as CoFe<sub>2</sub>O<sub>4</sub>/PZT, Ni<sub>0.75</sub>Co<sub>0.25</sub>Fe<sub>2</sub>O<sub>4</sub> + Ba<sub>0.8</sub>Pb<sub>0.2</sub>TiO<sub>3</sub> etc. Among these different composites BaTiO<sub>3</sub>-CoFe<sub>2</sub>O<sub>4</sub> composite seems to be most promising for applications. We therefore put the effort to study that system. Multiferroic BaTiO<sub>3</sub>-CoFe<sub>2</sub>O<sub>4</sub> composite could be regarded as model system illustrating magneto electric effect. BaTiO<sub>3</sub> is a typical ferroelectric material which has a large piezoelectricity. CoFe<sub>2</sub>O<sub>4</sub> is ferromagnetic with large magnetization. Wet chemical methods are coming into this field of particulate composite with a lot of advantages. Firstly the sintering temperature likely to be reduced as that is followed in conventional ceramic method. This will save electrical energy in processing. Playing with the properties with

varying compositions is also possible. Composite properties could be improved by proper mixing of constituents. Wet chemical method is very much helpful.

As a summary of some of the literatures which came across is tabulated as follows:

**TABLE 1:**

Serial no.	Name/group	Route followed to Synthesize $\text{CoZnFe}_2\text{O}_4$	Conclusions
1	S.D. Bhame, P.A. Joy	Conventional ceramic method, Combustion method, Citrate method, Coprecipitation method and	Lowest average grain size and highest magnetostriction is obtained for the material synthesized by an auto combustion method
2	R.W. McCallum, K.W. Dennis, D.C. Jiles, J.E. Snyder, Y.H. Chen	Auto Combustion method	High values of the strains at low field strengths along with enhanced magneto mechanical Coupling factor have been identified.
3	A. Goldman, T. Nakamura	Auto Combustion method	Exhibit improved magnetic permeability which depends on the microstructure, density, Porosity, grain size.

Table 1: Previous works on synthesis of  $\text{CoZnFe}_2\text{O}_4$



**TABLE 2:**

<b>Serial no.</b>	<b>Name/group</b>	<b>Route followed to Synthesize BaSrTiO<sub>3</sub></b>	<b>Conclusions</b>
1	A. Ianculescu, D. Berger, C. Matei, L. Mitoşeriu, E. Vasile	Citrate Gel Method	BaSrTiO <sub>3</sub> nano powders present various structural and morphological features depending on the type of raw materials
2	Sung-Soo Ryu , Sang-Kyun Lee , Dang-Hyok Yoon	Solid State Reaction Method	Reaction Temperature was decreased by doping Calcium
3	U.Manzoor, D.K.Kim	Solid State Reaction Method	Enhanced Reaction Rates due to increase in Contact area due to Small particles

Table 2: Previous works on synthesis of BaSrTiO<sub>3</sub>

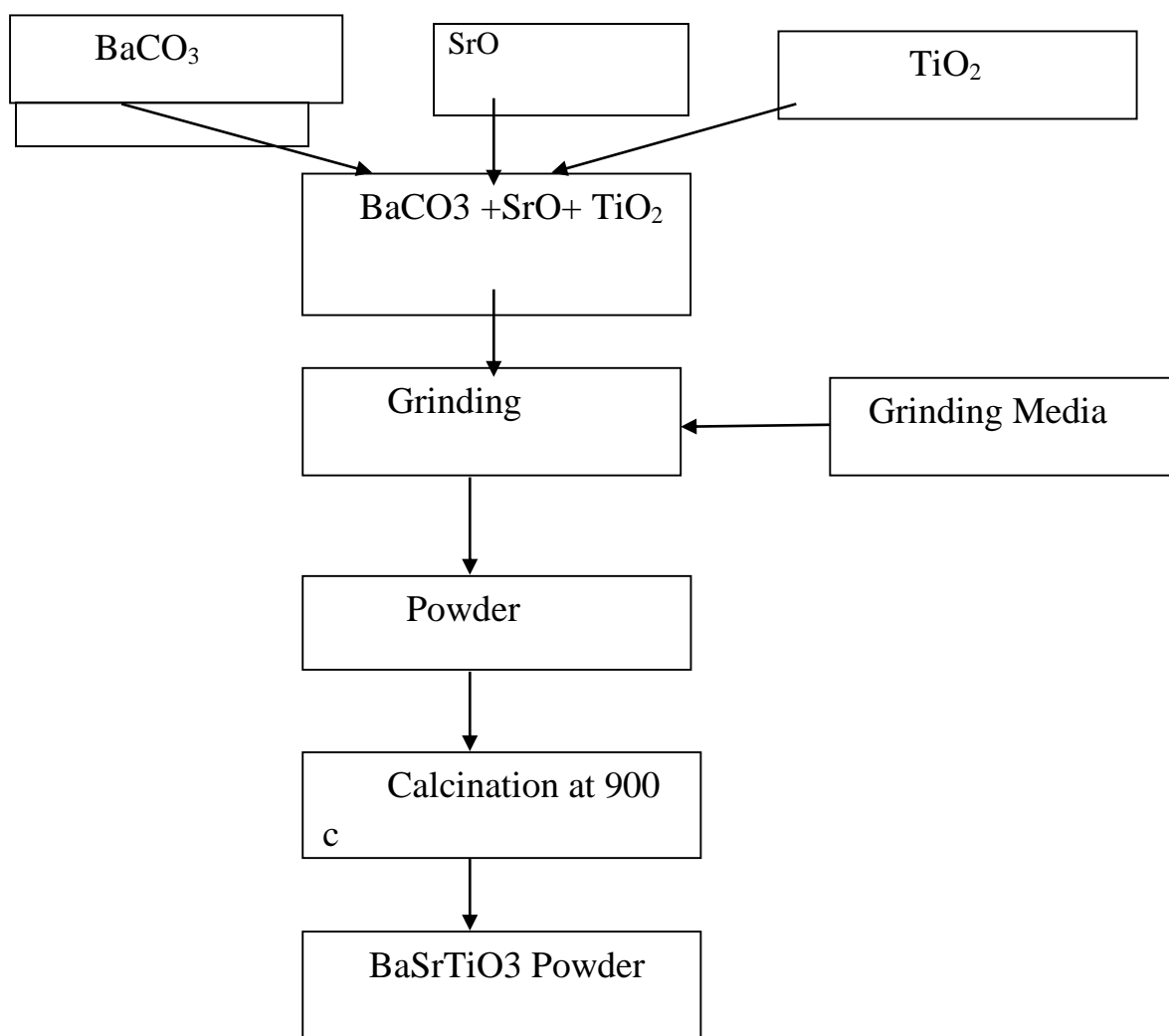
Chapter 3:

# **Experimental Procedure**

### 3.2 Preparation of BaTiO<sub>3</sub> Powder:

- **3.2.1 Dry Route:**

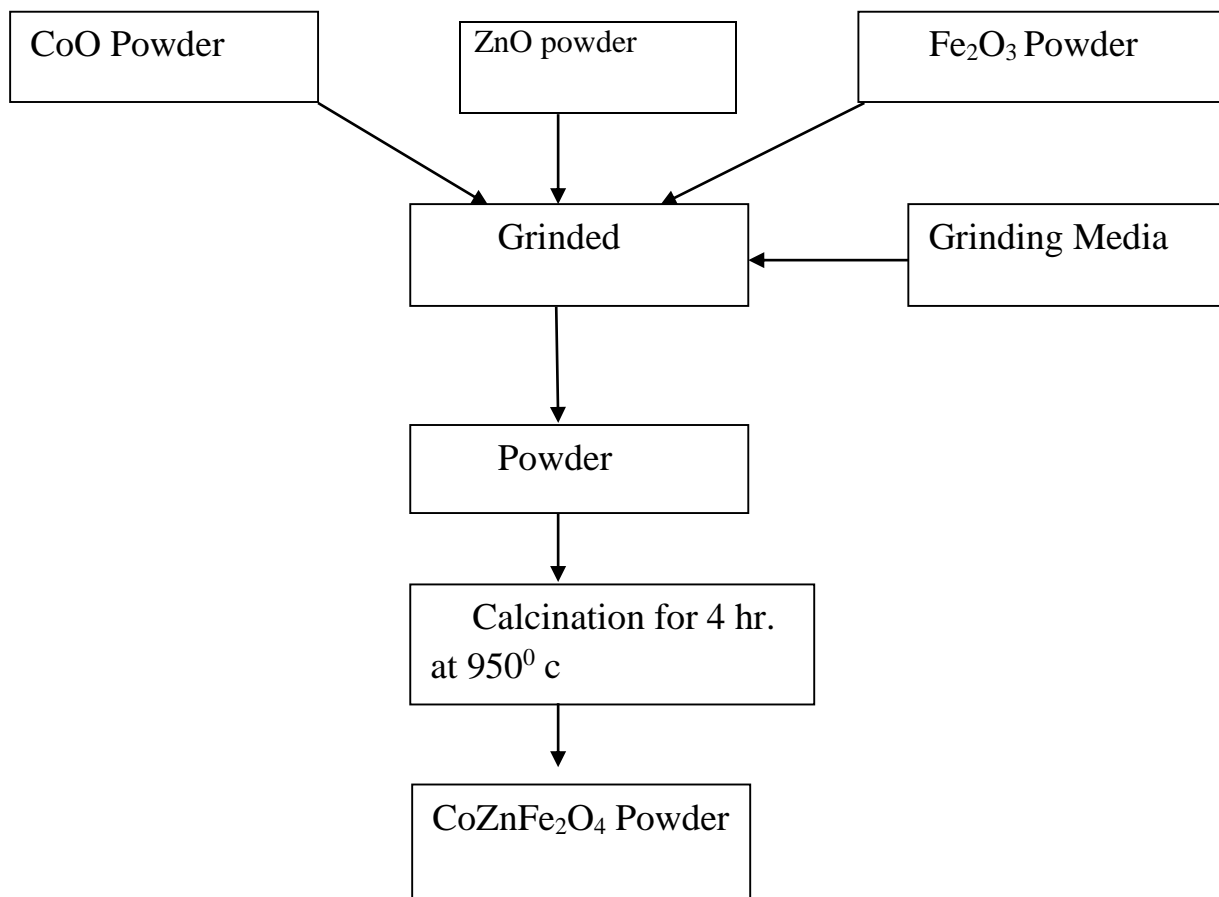
BaTiO<sub>3</sub> was prepared by the solid oxide route in which BaCO<sub>3</sub>, TiO<sub>2</sub> SrO was taken in 0.8:0.2:1 mole ratio and it was ground in the mortar for about 1 and a ½ hrs. with isopropyl alcohol as the grinding medium. Then the powder was calcined at 1000°C for 4 hrs and XRD was done to determine its phase.



Flowchart for Preparation of BaSrTiO<sub>3</sub> Powder by Dry route method

### 3. Cobalt zinc Ferrite Powder:

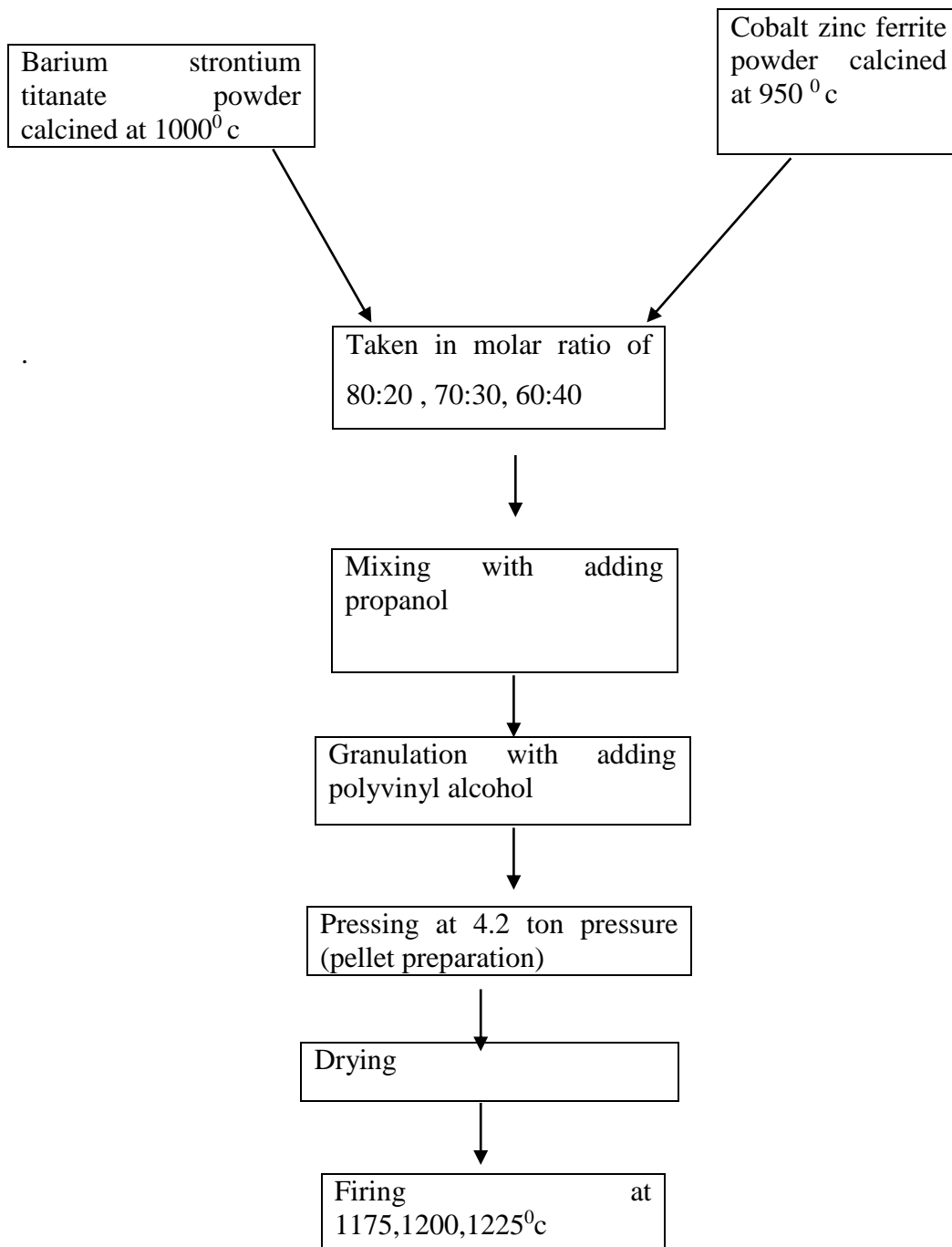
- 3.3.1 Dry Route:



Flowchart for preparation of Cobalt Ferrite Powder by Dry Route

Co<sub>0.8</sub> Zn<sub>0.2</sub> Fe<sub>2</sub>O<sub>4</sub> was also prepared by the solid oxide route in which Co<sub>3</sub>O<sub>4</sub>, ZnO and Fe<sub>2</sub>O<sub>3</sub> were taken in mole ratio of 0.8:0.2:1 and both were mixed and grounded for about 1 & ½ hrs. with acetone as the grinding media. The powder was then calcined at 950°C/4 Hour and its XRD was done to determine its phase.

Then desired sample are taken in the three molar ratio such as 80:20, 70:30, 60:40 of barium strontium titanate and cobalt zinc ferrite respectively which is described in the following table



The sample were fired at different temperature like 1150, 1175, 1200, 1225 °C, and sintering behavior was studied.

Then the characterization was studied like

- ✓ Apparent porosity
- ✓ Bulk density
- ✓ X ray diffraction
- ✓ FESEM
- ✓ Sintering behavior
- ✓ Dilatometer
- ✓ Magnetic property

# **Chapter 4:**

# **Results and**

# **Discussion**

## 4.1 X-ray diffraction analysis

### 4.1.1: Phase evolution of $\text{Ba}_{0.8}\text{Sr}_{0.2}\text{TiO}_3$ (abbreviated as BST) and $\text{Co}_{0.8}\text{Zn}_{0.2}\text{Fe}_2\text{O}_4$ (abbreviated as CZF)

As  $\text{Ba}_{0.8}\text{Sr}_{0.2}\text{TiO}_3$  (BST) and  $\text{Co}_{0.8}\text{Zn}_{0.2}\text{Fe}_2\text{O}_4$  (CFZ) are two constituent to study the composites, it was primary objective to obtain BST and CZF powder which are pure in physical phase. For BST, raw materials were taken as  $\text{BaCO}_3$ ,  $\text{SrO}$  and  $\text{TiO}_2$  in required amount to calcine at  $1000^\circ\text{C}/4\text{hr}$ . the same method was employed for CZF with strating materials  $\text{Co}_3\text{O}_4$ ,  $\text{Fe}_2\text{O}_3$  and  $\text{ZnO}_2$  where ther calcination temperature was chosen as  $950^\circ\text{C}$ . Phase evolution analyses of these powders were performed using the X-ray diffraction technique. Fig. 4.1 shows XRD patterns of solid state derived BST and powders using  $\text{BaCO}_3$   $\text{SrO}$  and  $\text{TiO}_2$  and calcined at  $1000^\circ\text{C}/4\text{hr}$ .

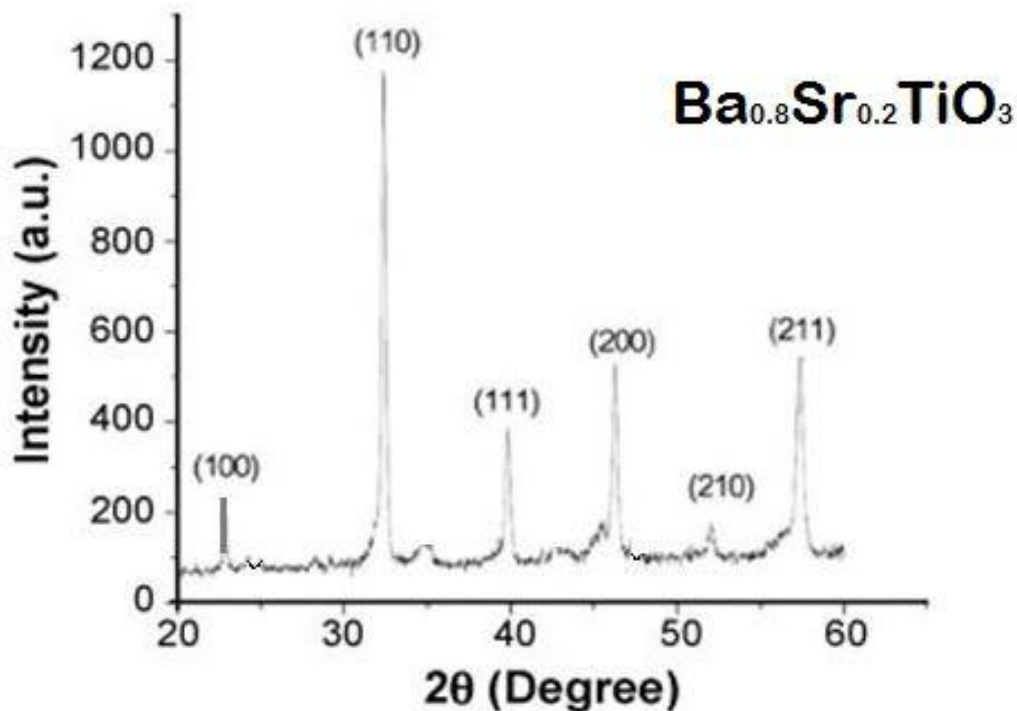




**Fig. 4.1: XRD graph of calcined BST prepared by solid state reaction (1000 °C)**

It was confirmed that cubic  $\text{Ba}_{0.8}\text{Sr}_{0.2}\text{TiO}_3$  was formed after calcination. For above pattern, peaks were found to be matched with reference pattern: 044-0093. The XRD pattern of calcined CZF has been represented in Fig. 2 to verify the fact whether there are impurity phases due to incomplete reactions or not. Sometimes intermediate compounds may form due to presence of impurities at the source. All impurities could be identified with XRD patterns.

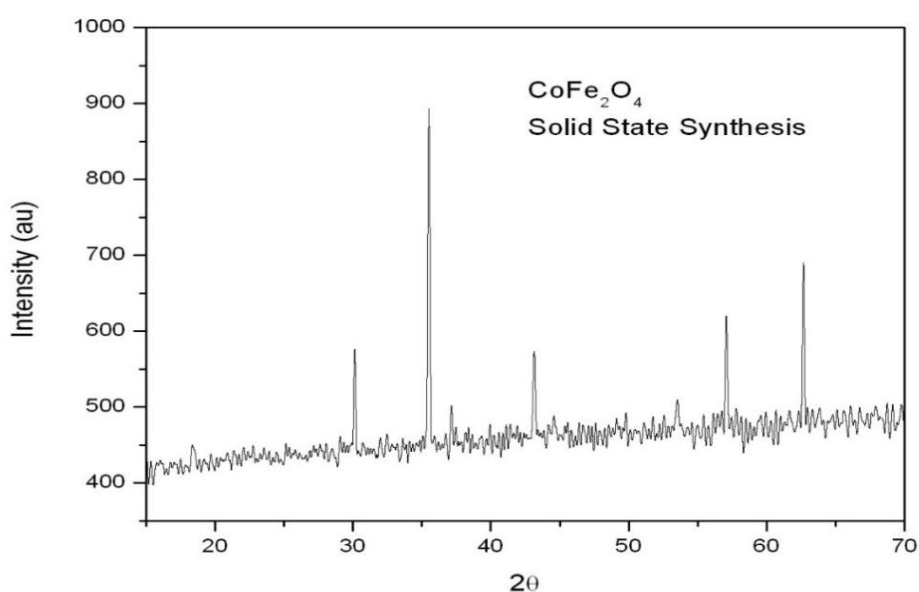


**Fig. 4.2: XRD graph of  $\text{Co}_{0.8}\text{Zn}_{0.2}\text{Fe}_2\text{O}_4$  synthesized by solid state reaction**

The pattern of calcined CZF is been matched with JCPDS pattern no. - 22-1086. No other impurity phases were found while matching with the reference pattern.

Thus phase pure BST and CFZ was obtained after calcination at 1000 and 950 °C respectively.

#### **4.1.2 X-ray Diffraction Analysis of sintered pellets**

Three Compositions are prepared with ideas from various literature which suggests that perovskite phase should be matrix where ferrite phase may vary from 20 to 50 mole percentage. Those compositions could be denoted by 0.6BST-0.2CZF, 0.7BST-0.3CZF and 0.8BST-0.2CZF with 60, 70 and 80 mole percentage of BST, where 40, 30 and 20 mole

percentage CZF is present respectively. All three compositions were subdivided into three subgroups. First batch represents the composite which actually got agate-mortar mixing only, second one got agate-mortar mixing followed by 15 minute dispersion by ultra-sonication and the third one got agate-mortar mixing and 30 minute dispersion by same sonication. Phase analysis was performed using XRD.

#### 4.1.2 [I] XRD of pellets sintered at 1175 °C (mixing in agate only )

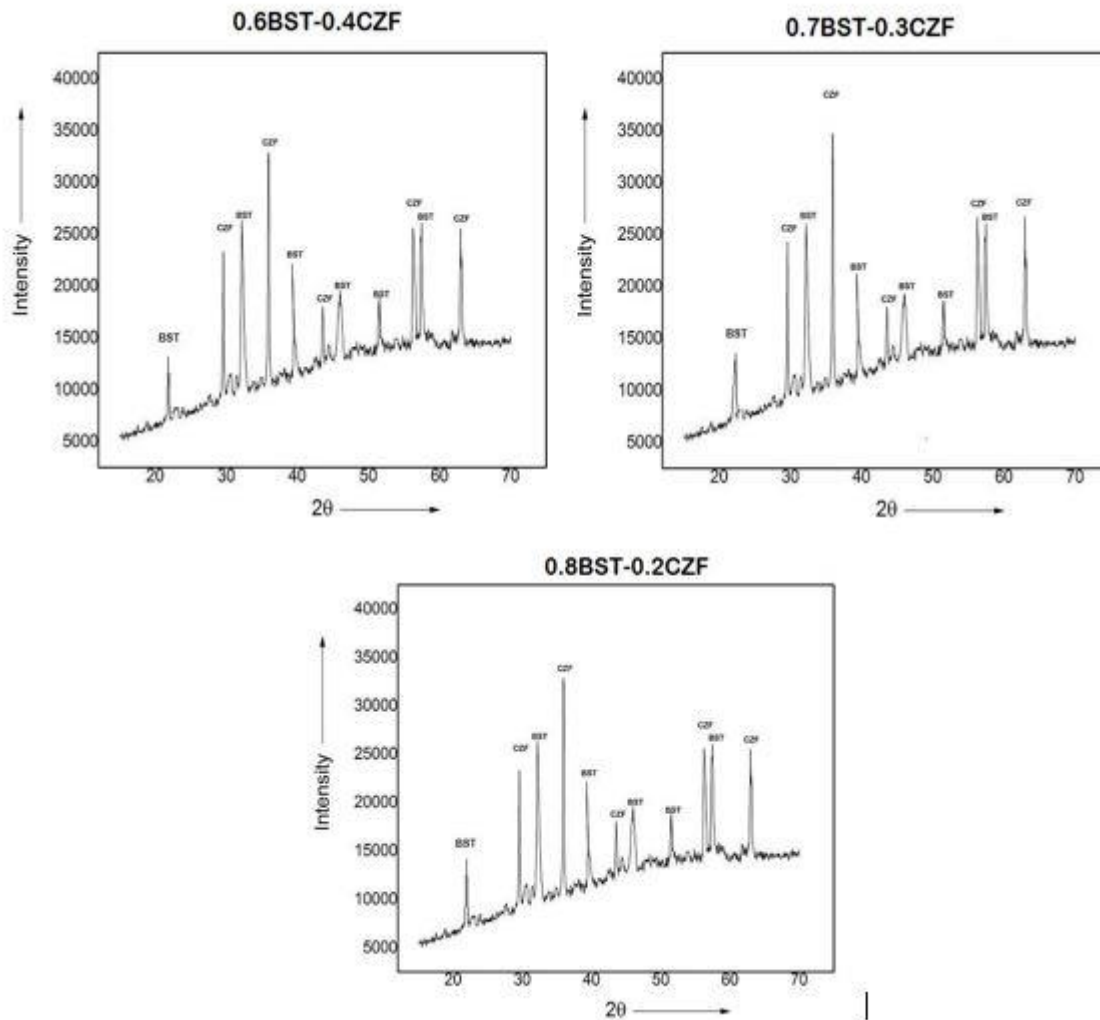


**Fig.4.3: XRD pattern of pellets after preparation from mixed batches**

#### 4.1.2 [II] XRD of pellets sintered at 1175 °C (mixing in agate +15 minutes sonication )

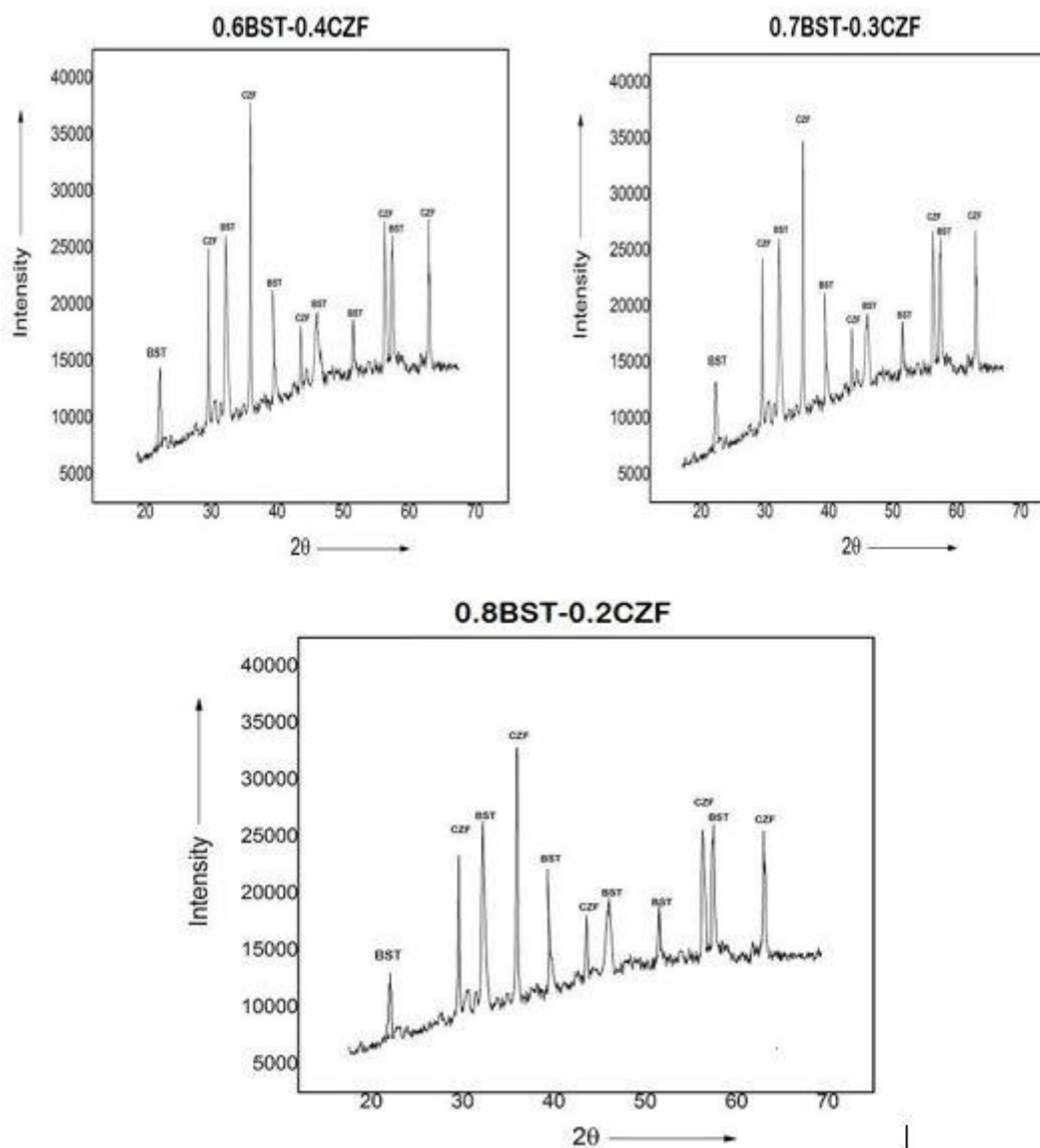


**Fig.4.4: XRD of pellets sintered at 1175 °C (mixing+15 minutes sonication )**

#### 4.1.2 [III] XRD of pellets sintered at 1175 °C (mixing+30 minutes sonication )

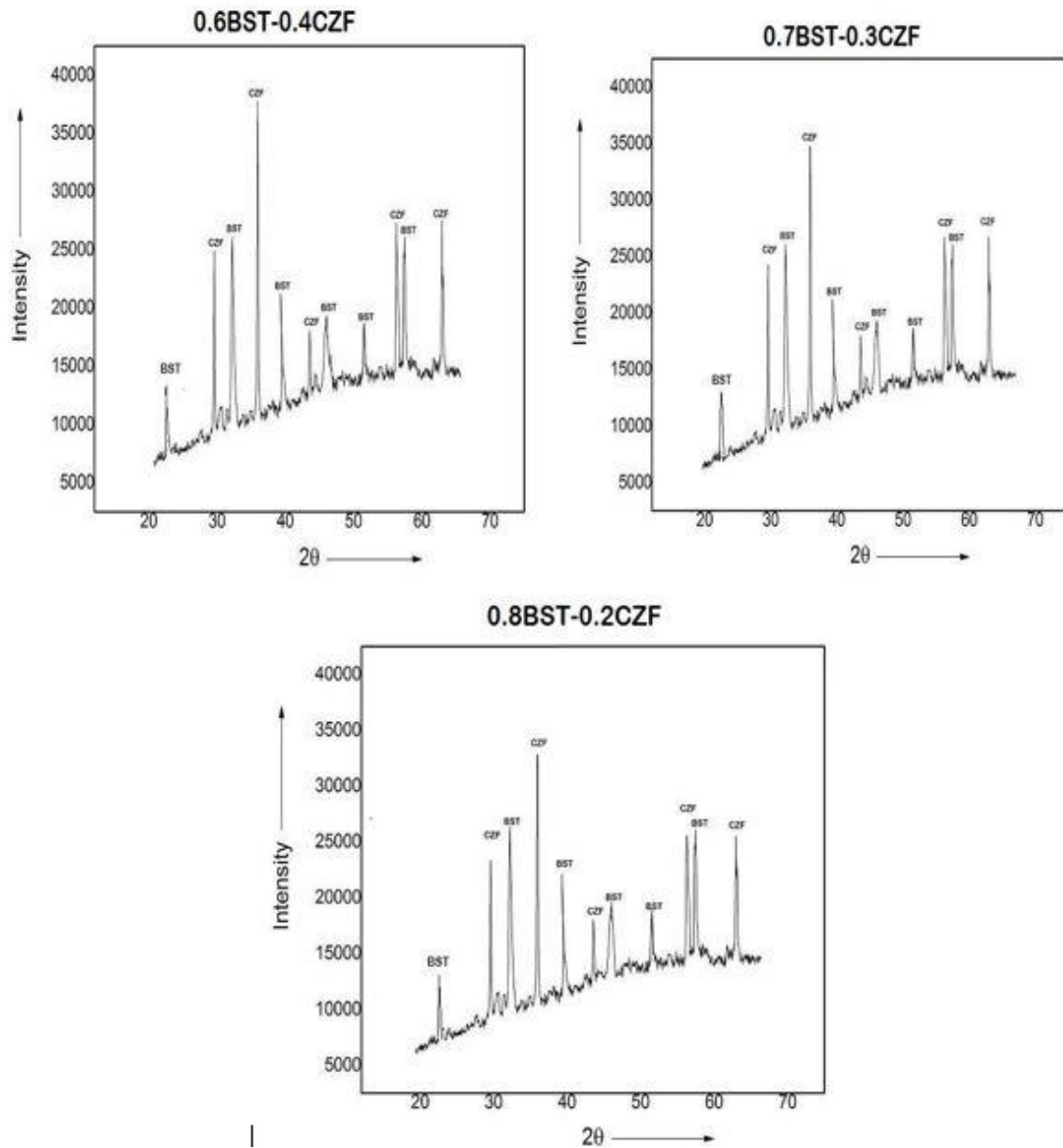


**Fig.4.5: XRD pattern of pellets after 30 min sonication**

## 4.2. Microstructure Analysis with Electron microscopy-images

Field-emission microscopy was employed to see the microstructure of the sintered composites. The followings are important regarding the microstructural analysis of samples.

(i) Phases should coexist maintaining the equilibrium. That means grains of BST and CZF should not give dissolution or melting after sintering. (ii) The NZF-phase distribution in the matrix of BST. In general more homogeneous distribution should ensure enhanced magnetic and ferroelectric properties.

### 4.2. [A] FE-SEM of as sintered (1175 °C/2hr) surface of composites ( agate-mortar mixing only )

Grain size ranges and the average grain sizes are calculated with a software name '*ImageJ*' by taking almost equal number of small medium and larger grainsizes. From the above microstructure the spherical grains were identified as BST and relatively larger are CZF. The information regarding grain size and grain size distribution are given in tabulation.

Electron-microscopy images were taken to observe the grain size and distribution of ferrites..

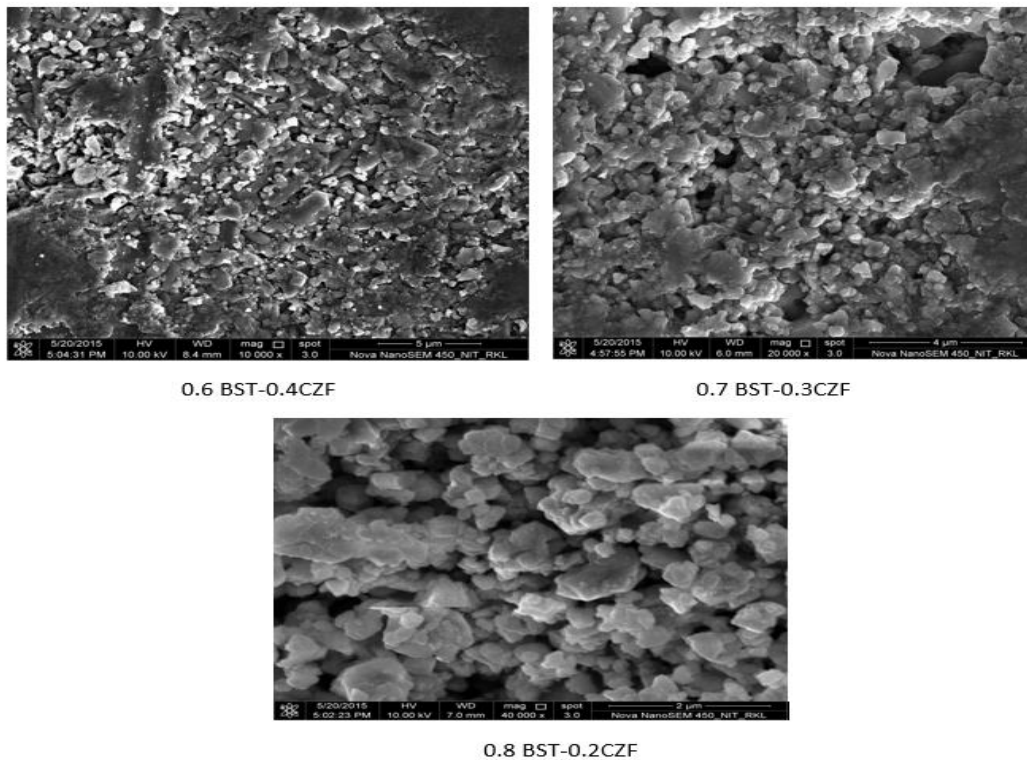


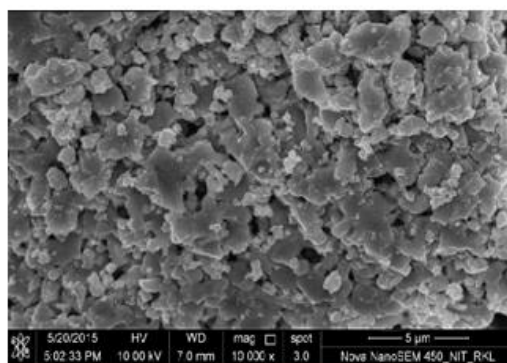
**Fig.4.6 FE-SEM images of 0.6BST-0.4CZF after 1175 °C/2hr (without sonication)**

**Table4.1: average grain size of BST and CZF**

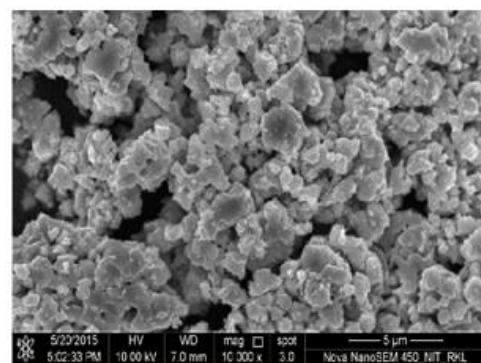
Composition	Grain size range ( $\mu\text{m}$ )	Average Grain size of BST( $\mu\text{m}$ )	Average Grain size of CZF ( $\mu\text{m}$ )
	BST CZF		
0.6BST-0.4CZF	0.33-0.84 1.23-2.5	0.59	1.902
0.7BST-0.3CZF	0.31-0.78 1.25-2.6	0.54	1.86
0.8BST-0.2CZF	0.28-0.86 1.31-2.8	0.51	1.76

#### 4.2. [B] FE-SEM of as sintered (1175 °C/2hr) surface of composites (mixing followed by 15 min sonication)

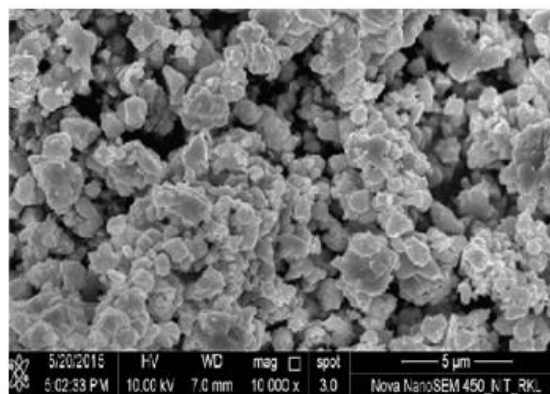
It was assumed that ultra-sonication would break the agglomerate and disperse BST so that there are more uniformity in ferrite phase distribution. The microstructures at below represents the figure that are microscopy images of the batches where 15 min sonication were done after mixing in agate.



0.6 BST-0.4CZF



0.7 BST-0.3CZF



0.8 BST-0.2CZF

**Fig.4.7 FE-SEM images of 0.6BST-0.4CZF after 1175 °C/2hr ( 15 min sonication)**

The important observations are tabulated as per below.

**Table 4.2 average grain size of BST and CZF of pellets (mixing in agate + 15 min sonication)**

<b>Composition</b>	<b>Grain size range BST CZF</b>	<b>Average Grain size of BST(<math>\mu\text{m}</math>)</b>	<b>Average Grain size of CZF (<math>\mu\text{m}</math>)</b>
0.6BST-0.4CZF 15 min	0.25-0.84 1.23-2.5	0.48	1.64
0.7BST-0.3CZF 15 min	0.22-0.78 1.25-2.6	0.45	1.63
0.8BST-0.2CZF 15 min	0.21-0.86 1.31-2.8	0.48	1.60

No such significant changes were observed except some smaller grains were appeared in microstructure. This may be due to breaking and dispersing of much finer grains.

#### **4.2. [C] FE-SEM of as sintered (1175 °C/2hr) surface of composites (mixing followed by 30 min sonication)**

Sonication time was doubled to see the effect of microstructural configuration. Instead of 15 mins that was accomplished with 30 mins dispersion. All three composition's secondary electron images were represented in below. One table has been given to see the average grain size of BST and NZF.

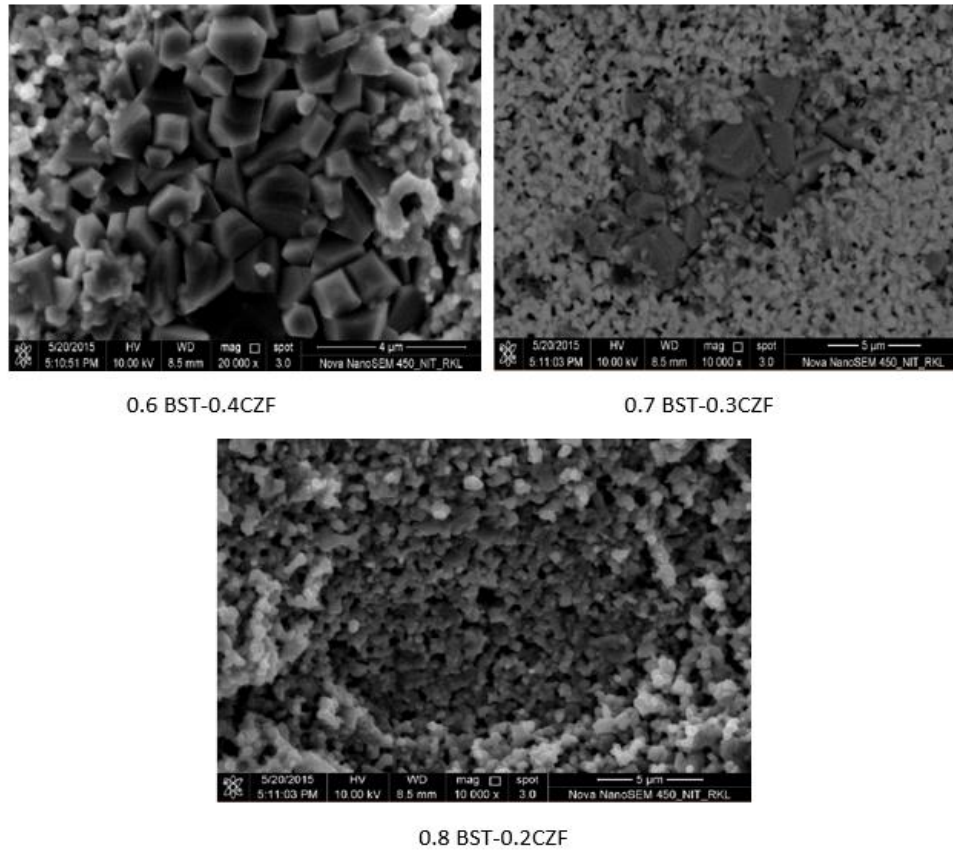


**Fig.4.8 FE-SEM images of 0.6BST-0.4CZF after 1175 °C/2hr ( 30 min sonication)**

**Table 4.3 average grain size of BST and CZF of pellets (mixing in agate + 30 min sonication)**

Composition	Grain size range BST CZF	Average Grain size of BST (μm)	Average Grain size of CZF (μm)
0.6BST- 0.4CZF 30 min	0.33-0.84 1.23-2.5	0.46	1.59
0.7BST- 0.3CZF 30 min	0.31-0.78 1.25-2.6	0.44	1.39
0.8BST- 0.2CZF 30 min	0.28-0.86 1.31-2.8	0.39	1.26

It could be concluded that the average grain size of BST came down significantly and that was much more visible in the composition 0.8BST-0.2CZF. although CZF sizes were kept unchanged with forming sort of colony. The impact of this kind of microstructure was



evident from B.D and A.P data. B.D. significantly rises due to fine microstructure of composites where 30 min sonication was followed.

#### 4.3. Bulk density (B.D.) and Apparent porosity (A.P.):-

##### 4.3. A Bulk Density (B.D)

Bulk Density determines the density of sintered product. The greater the B.D., the better of physical properties. The bulk density of the sample fired at 1175 °C. Are as follows:

**Table4.4: B.D. data of pellets sintered at 1175 °C/2hr**

<b>Average B.D. Composition</b> ↓	<b>Only mixing (gm/cm<sup>3</sup>)</b>	<b>Mixing + 15 min sonication (gm/cm<sup>3</sup>)</b>	<b>Mixing + 30 min sonication (gm/cm<sup>3</sup>)</b>
0.6BST-0.4CZF	4.33	4.40	4.48
0.7 BST-0.3CZF	4.57	4.62	4.69
0.8BST-0.2CZF	4.83	4.88	4.92

From the above table it was observed that B.D. value in all three compositions slightly increases. This may happen as ultra-sonication breaks the soft agglomerate and improves in packing with granules in dry pressing or green body compaction. The average increase was calculated as 3.44, 2.62 and 1.86 for the compositions 0.6BST-0.4CZF, 0.7BST-0.3CZF and 0.8BST-0.2CZF respectively.

##### 4.4. B Apparent Porosity (A.P.)

The apparent porosity of the pellet are as follows:-

**Table7: A.P. data of pellets sintered at 1175 °C/2hr**

<b>Average A.P. Composition</b> ↓	<b>Only mixing (Percentage, %)</b>	<b>Mixing + 15 min sonication (percentage, %)</b>	<b>Mixing + 30 min sonication (percentage, %)</b>
0.6BST-0.4CZF	4.30	4.26	4.21
0.7 BST-0.3CZF	4.1	3.98	3.91
0.8BST-0.2CZF	3.96	3.93	3.89

From the A.P. data represented at Table7, it could be said that apparent porosity varies with modification in processing, i.e., dispersing the composite powders with different time.

#### 4.4 Shrinkage behavior:

The experiment of shrinkage were accomplished in air atmosphere with a heating rate of 10 °C/min. the densification behaviour was important to discover the on-set temperature and the maximum temperature we should adopt for a composition. The following figure gives the shrinkage behaviour of three compositions mixed in agate without sonication.

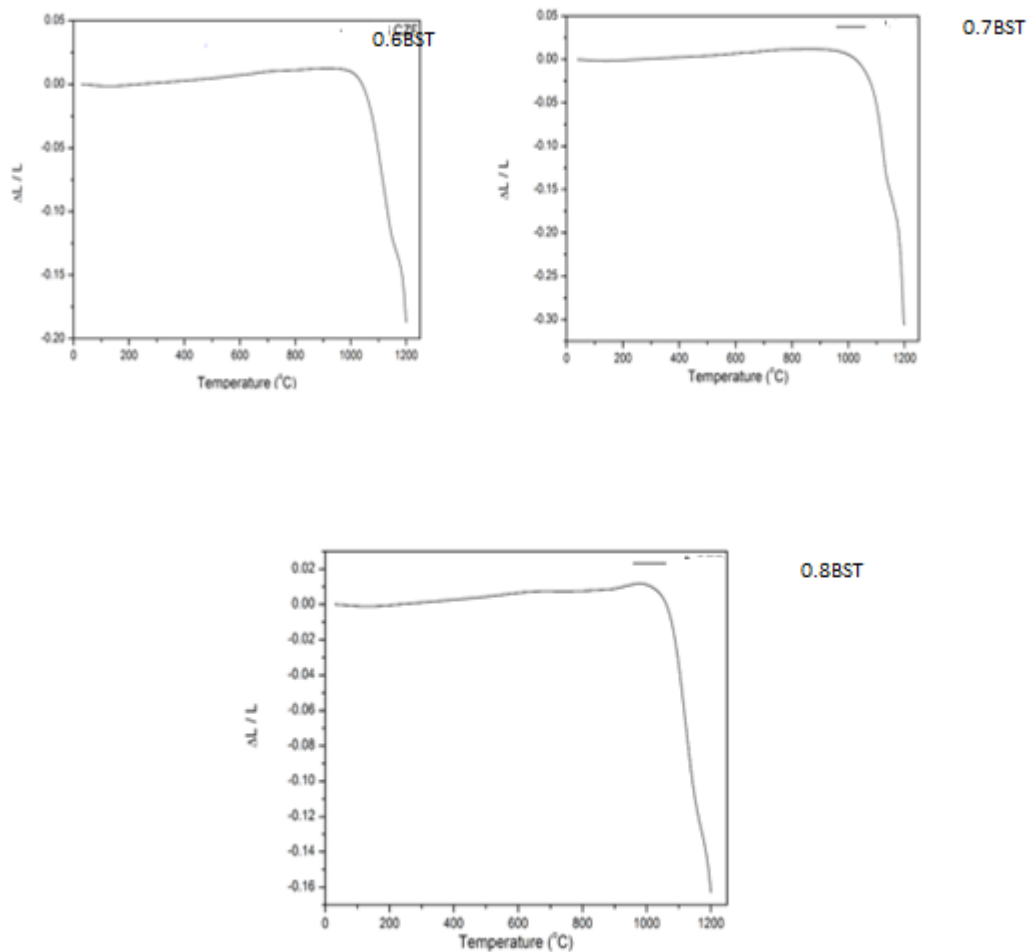


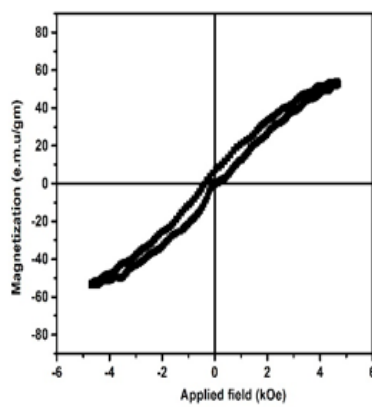
**Fig.4.9 dilatometric curve of three green compacted compositions**

From the above graph it can be found that the all the composition shows significant shrinkage beyond some temperature. The temperature at which shrinkage increases significantly is known as on-set temperature. So as the ferrite % decreases the maximum temperature at which the shrinkage occur increases due to formation of eutectic. The on-set temperature of densification was seen to be composition dependent. The following table at below exhibits the corresponding temperature.

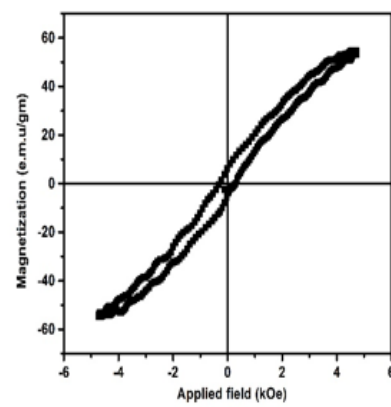
**Table 4.5: Onset temperature of densification ( $^{\circ}\text{C}$ ) mixed in agate only**

Composition	Onset temperature of densification ( $^{\circ}\text{C}$ )
0.6 BST-0.4CZF	1040.26
0.7 BST-0.3CZF	1026.96
0.8 BST-0.2CZF	1060.10

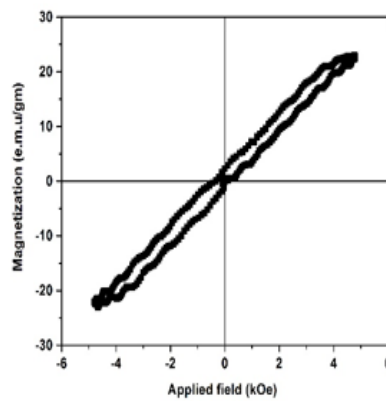
#### 4.5 Magnetic properties:-



0.6BST 0 min sonication

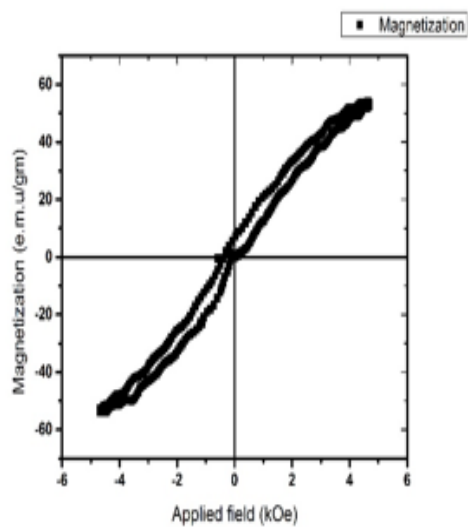


0.7BST 0 min sonication

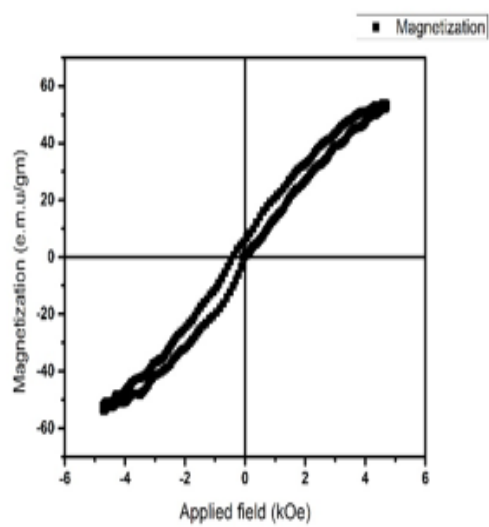


0.8BST 0 min sonication

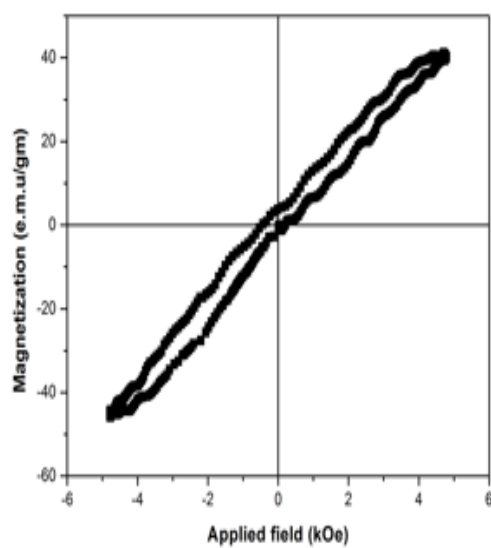
**Fig 4.10 B-H loops of three composites only mixed in agate**



0.7BST 15 min sonication

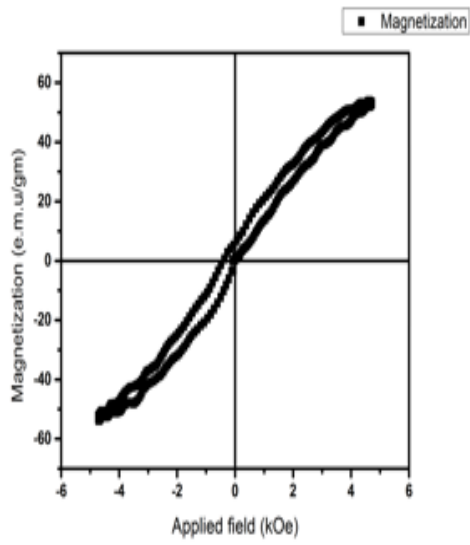


0.7BST 15 min sonication

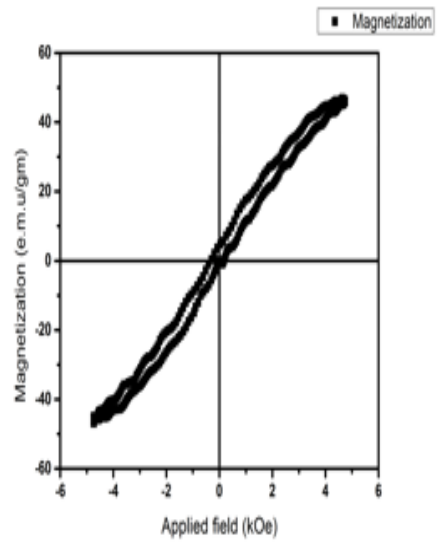


0.8BST 15 min sonication

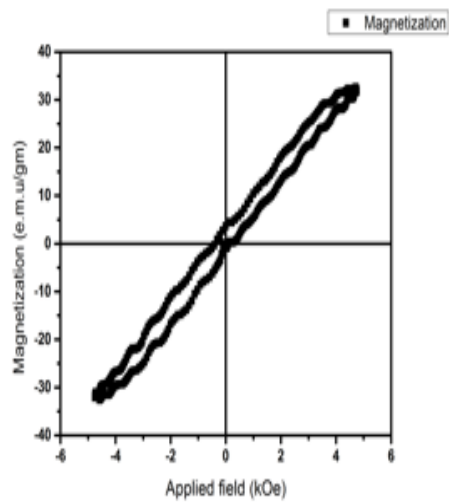
**Fig 4.11 B-H loops of three composites mixed in agate followed by 15 min dispersion**



0.6BST 30 min sonication



0.7BST 30 min sonication



0.8 BST 30 min sonication

**Fig 4.12 B-H loops of three composites mixed in agate followed by 30 min dispersion**

**Table 4.6. Magnetic order parameters as obtained from B-H loops**

<b>Composition</b>	<b>Saturation magnetization(<math>M_s</math>) (e.m.u/gm)</b>	<b>Remainant magnetization(<math>M_r</math>) (e.m.u/gm)</b>	<b>Coercive field(kOe)</b>
0.6 BST-0.4CZF 0 min sonicated	54	6.5	0.48
0.6 BST-0.4CZF 15 min sonicated	54	6.89	0.5
0.6 BST-0.4CZF 30 min sonicated	55	6.92	0.51
0.7 BST-0.3CZF 0 min sonicated	48	6.8	0.42
0.7 BST-0.3CZF 15 min sonicated	49	5.01	0.40
0.7 BST-0.3CZF 30 min sonicated	49	5.00	0.4
0.8 BST-0.2CZF 0 min sonicated	27	4.5	0.38
0.8 BST-0.2CZF 15 min sonicated	36	7.00	0.38
0.8 BST-0.2CZF 30 min sonicated	41	4.5	0.6

The magnetic property were determined and studied. It shows that as the cobalt zinc ferrite concentration increases the magnetic character increases i.e. the saturation magnetisation, remainnant magnetisation and coercive field increases. The properties are better when they are sonicated. The highest saturation magnetisation is 55 e.m.u/gm observe in 0.6BST-0.4CZF sonicated at 30 min.

### Ferroelectric property:-

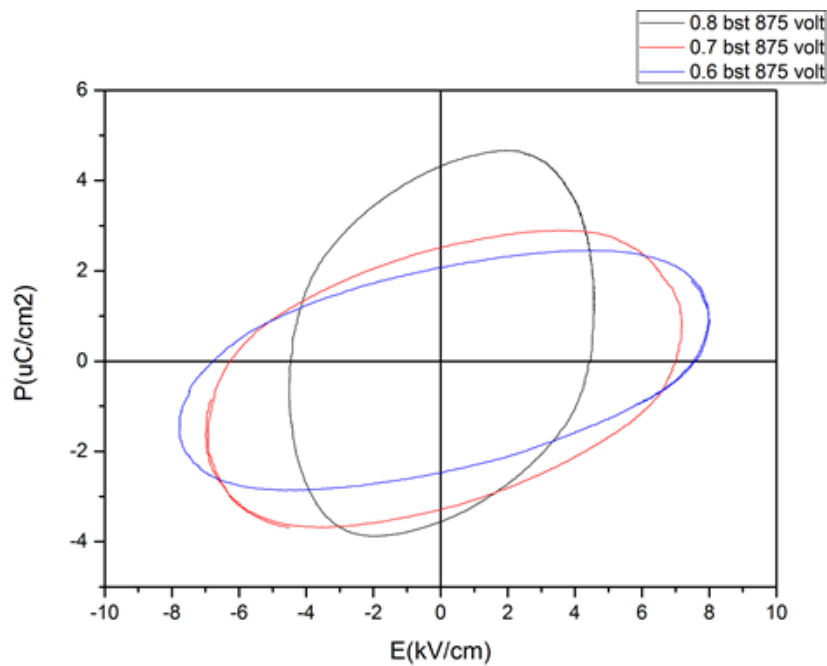


**Fig 4.13 P-E loops of three composites mixed in agate only**

The figure shows the ferroelectric orders are present. BST phase is able to produce that characteristic. The details are reported in following.

**Table 4.7: Ferroelectric order parameters as obtained from P-E loops**

Composition	Remainant polarization ( $\mu\text{C}/\text{cm}^2$ )	Maximum polarisation( $\mu\text{C}/\text{cm}^2$ )
0.6BST-0.4CZF	1.8	2.4
0.7BST-0.3CZF	2.3	2.8
0.8BST-0.2CZF	4.2	4.8

# **Chapter 5:**

# **Conclusions:-**



- As the phases have been confirmed by XRD these samples can be used for preparation of magneto electric composite
- From the FESEM we got that on increasing the ferrite content the agglomeration of the particles takes place.
- On increasing the BST the ferroelectric properties increases quite significantly and on increasing the CZF the magnetisation increases.
- From the XRD the peak are confirmed and some peaks are due to impurity phases.
- On decreasing the CZF the apparent porosity and bulk density increases significantly as the pure BST has the density around 5.88
- On sintering above 1200 deg cel. The liquid phase developed significantly and the sample began to melt so firing was done at 1175 °C.
- All the property were better for the case of sonicated sample like AP, BD, FESEM ferroelectric and magnetic measurement as fine dispersion of particle takes place in sonication.

# **Chapter 6:**

# **References**

1. Goldman, Modern Ferrite Technology, Van Nostrand Reinhold, New York, 1990.
2. T. Nakamura, J. Magn. Magn. Mater. 168 (1997) 285
3. R.W. McCallum, K.W. Dennis, D.C. Jiles, J.E. Snyder, Y.H. Chen, Low Temp. Phys. 27 (2001) 266.
4. . D.H. Yoon, B.I. Lee, J. Ceram Process. Res. 3(2), 41 (2002).
5. J. Ryu, S. Priya, K. Uchino, H.E. Kim, D. Viehland, J. Korean Ceram. Soc. 39 (9) (2002) 813–817.
6. Multiferroic and magnetoelectric materials, W. Eerenstein, N. D. Mathur & J. F. Scott 2006.
7. U.Manzoor and D.K.Kim: Scripta Mater., 2006, 54, 807.
8. A. Ianculescu, D. Berger, M. Viviani, C.E. Ciomaga, L. Mitoşeriu, E. Vasile, N. Drăgan, D. Crişan, J. Eur. Ceram. Soc., **27**, 3655 (2007)
9. Structural analysis and electrical properties of ME composites, S.A. Lokare, R.S. Devan, B.K. Chougule, 2007
10. The physics of magnetoelectric composites R. Großsinger,\_, Giap V. Duongb, R. Sato-Turtellia, 2007